Applying Peg-in-Hole Actions with a Service Robot

Stefan-Daniel Suvei[1], Leon Bodenhagen[1], Thomas Nicky Thulesen[1], Milad Jami[2]
and Norbert Krüger[1]
[1]*University of Southern Denmark, 5230 Odense M, Denmark*
[2]*Novo Nordisk A/S, Novo Alle, 2880 Bagsvaerd, Denmark*

Keywords: Service Robot, Peg-in-Hole, Simulation.

Abstract: A general requirement for any service robot is to be flexible and capable of processing uncertainties, thus making it adaptable for multiple tasks. As a result, learning the appropriate action parameters for a specific action is a crucial task. The method presented in this paper is an incremental statistical learning method that takes into consideration the uncertainties and the contact forces to find the optimal parameter sets. The method is inspired by solutions available in industrial robotics and it uses a dynamic simulator and Kernel Density Estimation in order to find the parameter sets that lead to a successful Peg-in-Hole action. The solution obtained in the simulation is successfully tested on a real service robot.

1 INTRODUCTION

In industry, robotic solutions are well established. One reason that facilitates the application of these solutions is that the environment can be controlled, such that uncertainties and thereby error sources are minimized. Current approaches focus on enabling robots to solve tasks despite of uncertainties. Solutions for handling uncertainties in e.g. assembly processes include online pose estimation of relevant items (Schwarz et al., 2015), use compliant manipulators (Kashiri et al., 2014) or utilize re-planning (Mainprice et al., 2015).

Within the domain of service robotics, the problem of correctly handling uncertainties is crucial, in particular when considering the fact that service robots have to work in unstructured and dynamic environments where they need to assist or work alongside humans. The challenge is to apply some of the well-tested industrial solutions in the service robotics field. This is due to the fact that safety, the ease of use and the flexibility are important aspects that need to be considered when talking about a service robot.

A good example of a process that can be transferred into service robotics from the industry and in which uncertainties can create big challenges is the classical tight fitting Peg-in-Hole (PiH) process (Dietrich et al., 2010),(Lin et al., 2014). Viewed mostly as an industrial, assembly type of task, many tasks in the field of service robotics such as collecting bottles, disposing of trash or inserting cutlery into the dishwasher compartiments can be consider to be PiH actions.

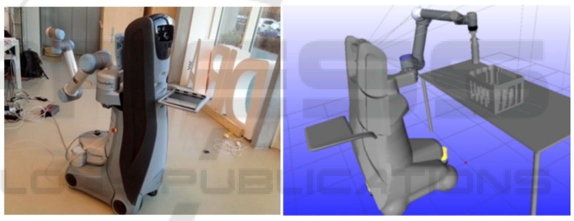
Figure 1: Care-O-Bot architecture. Left: Real platform. Right: Simulated platform.

Manually tuning the parameters that normally define the PiH action is challenging, since there is no guarantee that the selected solution will be successful for each trial. Sensor-controlled actions can be used to handle this type of situations, however, this generally leads to an increase in the overall process-time and cost.

Another approach is to use action parameter optimization techniques to reduce the number of samples in the search space, like in (Sørensen et al., 2016), where Kernel Density Estimation is used during the learning phase to eliminate the sub-optimal areas of the search space. This is done by considering the result of the experiments in the surrounding neighborhood.

Our proposed method makes use of a dynamic simulator and Kernel Density Estimation to do a postlearning search through the parameter space and find those sets that lead to a successful Peg-in-Hole action. In order to eliminate unpromising parameter sets, process uncertainties and the appearance of contact forces are taken into consideration. The result is tested and verified on both a simulated and a real platform.

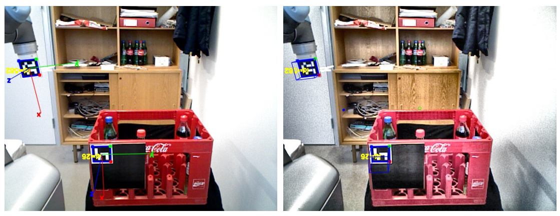
(a) Original RGB data (b) Modified RGB data

Figure 2: Visualization of the Aruco traker output - the two markers are detected and the transformations between them and the camera are computed.

2 RELATED WORK

With the rise of interest for service robotics, classical robotic topics such as safe planning, visual servoing and manipulation have recently regained focus, with the goal of adapting some of the well-known industrial methods to the more challenging home environment. Action-parameter learning, in particular, has been of great concern, specifically because it is applicable to a large array of tasks, thus increasing the flexibility of the system. The learning process can be done using the execution feedback data received from the sensors and adapting the action process according to the found environment constraints (Gams et al., 2014), (Berio et al., 2016), by human demonstration (Gams and Petrič, 2016) or by using dynamic simulation, thus facilitating an extended exploration of the parameter space (Jørgensen and Petersen, 2008), (Detry et al., 2011), (Sørensen et al., 2016).

As opposed to industrial robots, service robots have to be flexible in order to function in unstructured and dynamic environments. As such, a rigid calibration of the tested setup is not a viable solution. For systems that are required to manipulate the environment and are equipped with a camera, a way of overcoming this issue is through position based visual servoing (PBVS) (Cherubini et al., 2008). This method uses the difference between the pose of the desired target object and that of the manipulator to determine the control error. For the target object, the pose estimation can be determined by using a 3D model of the object and the homography, like in (Kyrki et al., 2004). (Gratal et al., 2011) proposes an alternative solution, by using a real-time model-based tracking method to estimate the pose of the gripper.

Compared to other approaches, we address the PiH task of inserting bottles into a crate using a service robot, for which no special calibration, specific environment manipulation (i.e. light adjustment, position control, etc.) or additional sensors (such as force-torque sensors or compliant grippers) are used. PBVS and dynamic simulation are utilized in order to achieve the task with minimum contact force. The parameter set that describes the tested PiH action, alongside the actual action path are determined in simulation. We demonstrate that the solution found in simulation can be directly used on a real platform, where the PiH action is not only successful, but also generates low contact forces.

3 EXPERIMENTAL SETUP AND METHODOLOGY

The Care-O-Bot (Graf et al., 2009) is a robotics platform that was developed to be a mobile robot assistant that actively supports humans in domestic environments. A big advantage of the Care-O-Bot platform (see Figure 1) is that it is equipped with multiple sensors and has a modular hardware setup, which makes it fit for a large array of tasks, such as: pick-and-place, object detection, human tracking, etc. The main components of the Care-O-Bot are: the omnidirectional mobile base, an actuated torso with 3 DoF, the UR5 robotic arm, the UR connector (to which the arm is attached), the tray, the head (which contains a Carmine 3D Sensor and a high resolution stereo camera) and three laser scanners. Using this platform, we investigate the possibility of solving a PiH task that consists of inserting bottles into a crate and learn the best parameter sets that define this action.

3.1 Tracking and Visual Servoing

The PBVS method determines the error between the pose estimation of the end effector and that of the desired object (in this case, the bottle crate) and uses it as a control error, in order to move the arm towards the desired position. As follows, the control loop is an endpoint closed loop, where both the end effector and the crate are in the field of view.

To ease the process of pose estimation and tracking, two AR (Augmented Reality) markers, denoted M1 and M2 in the following, are attached to the gripper and the bottle crate. With the help of the ”aruco_ros” ROS tracker (Garrido-Jurado et al., 2014), the markers are detected and the transformation between them is determined. The obvious downside of this approach is that the markers must constantly be detectable by the camera, which makes it sensitive to the illumination level in the environment, specifically since the robot was placed in a laboratory with a lot of natural light. To overcome this issue, we apply the Contrast Limited Adaptive Histogram Equalization algorithm (Zuiderveld, 1994) on the input RGB image data of "aruco_ros" tracker, thus improving the overall contrast of the image, as can be seen in Figure 2, and aiding the corner detection.

The two transformations are used in a classic linear interpolation algorithm that generates the incremental displacements that will move the robotic arm with the end effector towards the crate and decrease the pose estimation error between the two AR markers.

The algorithm is repeated until the Euclidean distance between the two markers is smaller than a predefined threshold which will ensure that the gripper is placed above the crate. To avoid overshooting this position, the incremental displacements decrease as the Euclidean distance between the markers decreases. Once the desired position is reached, the algorithm updates the position of the crate based on a final reading of the M2 marker and then starts the Peg-in-Hole action sequence.

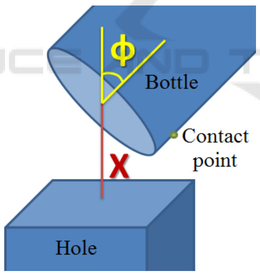

Figure 3: The PiH action parameters.

3.2 Action Parametrization

The Peg-in-Hole action in our context is defined by two parameters (Figure 3) and is performed in four steps (Figure 4). The parameters span the search space and are defined as follows:
***x*:** The perpendicular distance between the hole and the middle of the bottle bottom.
ϕ: The angle of the bottle in the initial position relative to the hole vertical axis.

If we assume an ideal PiH action (i.e. no uncertainties), the four steps that compose the action as a whole are described as follows:
Initial Position: In the first step the robot moves the bottle from the position where it was left by the visual servoing algorithm towards the hole. At the end of this motion, the bottle is at a perpendicular distance of $5\,cm$ from the hole and tilted with an angle ϕ.
First Linear Motion: In the second step, the bottle is moved linearly towards the hole (Figure 4(a)). The movement stops when the end of the bottle is at a perpendicular distance X above from the hole. At this point, the bottle is touching the edge of the hole.
Circular Motion: After the first linear movement and the contact with the hole's edge, the bottle is rotated until $\phi = 0$, as depicted in Figure 4(b).
Second linear Motion: In the final step, the bottle is moved linearly down the hole and the bottle's axis is kept aligned with the hole (Figure 4(c)). In our proposed solution, when the bottom of the bottle is inside the hole after the second linear motion, the robot just drops the bottle into the hole.

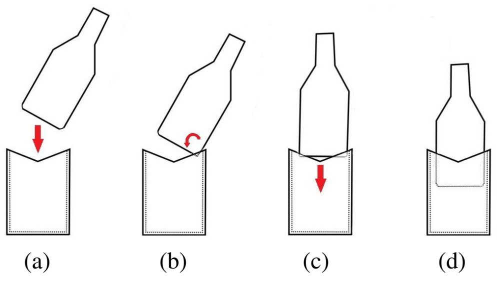
Figure 4: The PiH action movements: (a) First linear motion. (b) Circular motion. (c) Second linear motion.
(d) Final position.

The PiH action is evaluated after the second linear motion. For a successful action, the bottle has to be partially inside the specified crate hole, such that a simple release of the gripper would drop it in the hole (see Figure 4(d)). This is confirmed by checking the pose of the bottle with respect to the hole. In the case in which the bottle gets stuck by hitting the edge of the hole, the action is labeled as a failure.

Using the described steps, the relative path between the bottle and the hole is computed for each parameter set. This path is then executed in both the simulated environment and on the real world setup. The evaluation and labeling of the action (i.e. success of failure) is done automatically in simulation and manually for the real world platform.

3.3 Action Simulation

The action simulation is performed using different values for the action parameters. The ranges of the parameters are set beforehand and define the search space. As such, the action is simulated within the parameter ranges of $x \in [-3;3]\,cm$ and $\phi \in [-45;45]^{\circ}$,

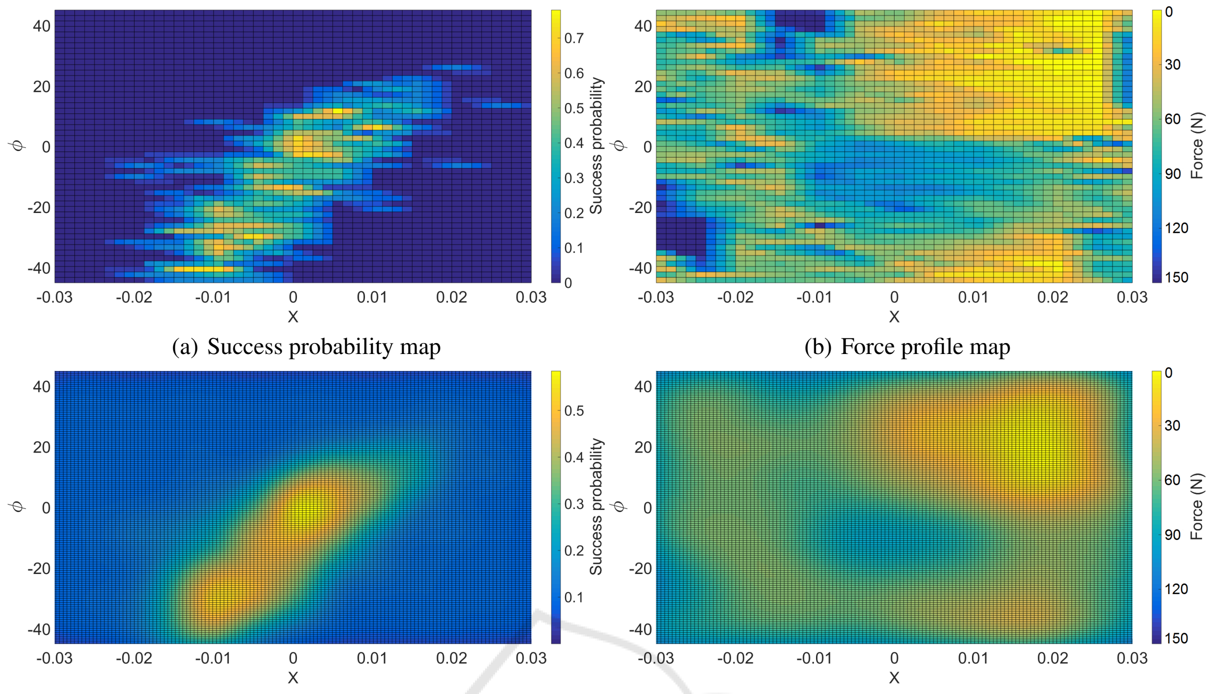

(a) Success probability map (b) Force profile map

(c) Success probability map KDE (d) Force profile map KDE

Figure 5: The success probability map and the force profile map before and after KDE.

with step sizes of 5 *mm* and 2° respectively.

To allow the learning sequence to deal with uncertainties, positional and rotational noise is added to the bottle frame and the hole frame in the action simulation. This is done by randomly choosing a direction from the XYZ-axes and multiplying it with a random value from a normal distribution to the chosen direction. For the crate, the normal distribution has a mean value of zero and a standard deviation of $3.5\,mm$ for the position and 3° for the rotation. For the bottle, the standard deviation is $1\,mm$ and 0.5° for the positional and the rotational noise respectively. The ranges of the uncertainties are based on the geometric models of the bottle and crate used in the simulator and on preliminary simulation tests. Due to the fit of the bottle and the hole, any positional error larger than $2.5\,mm$ on one of the XY-axes or a rotational error larger than 0.8° on one of the PY-Euler angles will result in the bottle getting stuck on the edge of the crate or applying forces on the crate, as observed in initial simulation tests.

3.4 Action Learning

To learn the parameter values that will lead to a successful task, the action is simulated 5 times for each pair of parameters, where the perturbation for each pair of samples is randomly selected as explained in the previous paragraph. This leads to a total number of 2925 individual tests of the PiH action. The results are visualized using a success probability map as in Figure 5(a).

To further narrow down the solution parameter space, we also investigate the force profile of the actions. For each parameter set, the average of the highest contact forces that characterized each repetition is computed. A threshold is used to limit the maximum allowed force to $150\,N$. The forces distribution can be seen in Figure 5(b). We note that the measured contact force is between the bottle and the hole for which the insertion is tested. For this reason, in the upper-right corner of the map, where the bottle is colliding with the crate (but not with the actual hole edges) it seems that there are little to no contact forces.

The next step is to multiply the Kernel Density Estimations of the success probability map and of the forces distribution, in order to choose a set of parameters for which the action would be successful, while at the same time the contact force between the bottle and crate would be minimal. The result (seen in Figure 7) is further discussed in section 4.1.

4 RESULTS

In this section, we show how by applying KDE on the results of the Action Learning sequence, we can

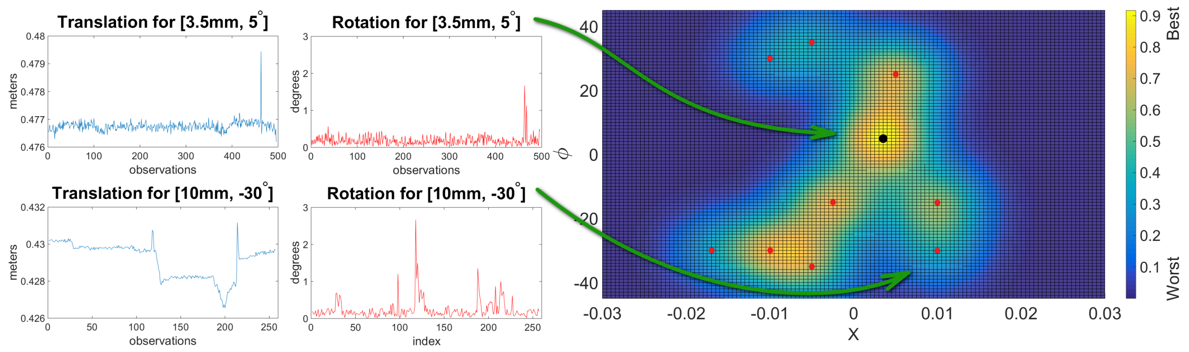

(a) Real world experiment

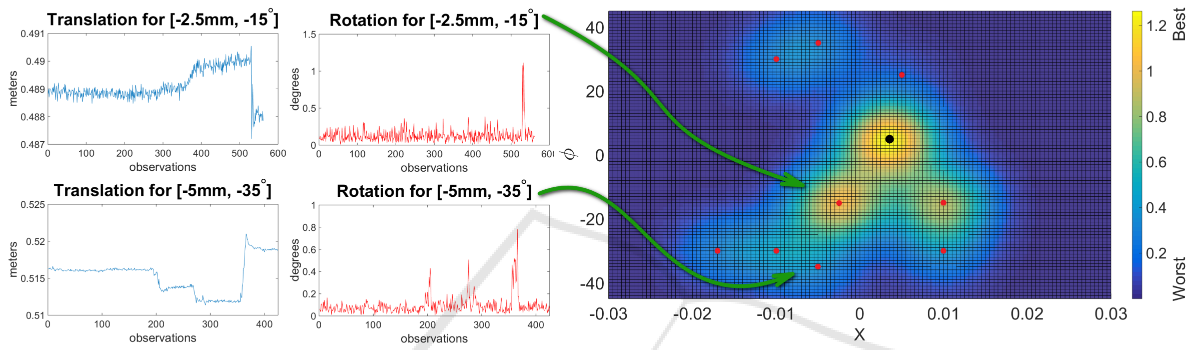

(b) Real world experiment with added noise

Figure 6: The KDE representation of the success and force profile of the 10 tested parameter sets. The parameter sets are marked with the red dots. The best set is marked with the black dot.

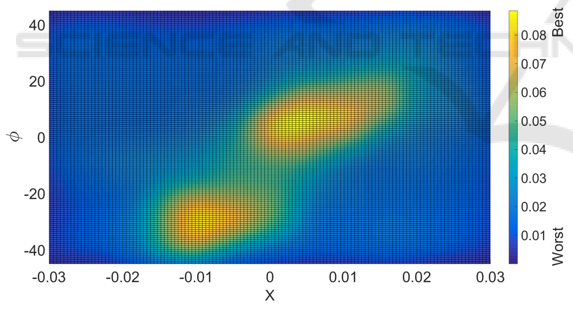

Figure 7: The multiplied KDE representation of the success and force profile.

reduce the parameter space and find good parameter sets that would yield a successful PiH action. We further test a subset of the parameters on the real platform and compare the result with the simulated ones.

4.1 Optimal Actions in Simulation

As mentioned in section 3.4, Kernel Density Estimation is used for both the success probability (Figure 5(a)) and the force profile map (Figure 5(b)) to get a good overview of the structure of the data and a good approximation of the best parameter sets.

The Matlab implementation of the KDE via diffusion method (Botev et al., 2010) is used, in which we use a multivariate Gaussian kernel and we define each independent data sample as a vector of type $s = [x;\phi;d]$, where x and ϕ are the two PiH action parameters and d is either the success probability or the force value for that specific parameter set. The value of d is the one that decides the smoothing contribution of each specific $[x,\phi]$ parameter set. In this specific Matlab implementation, the kernel density is estimated based on the smoothing properties of linear diffusion processes. If we consider $(s_1, s_2, \ldots, s_n)$ independent samples from an unknown continuous probability function f, then the kernel density estimator is defined as:

$$\hat{f}(s) = \frac{1}{nh}\sum_{i=1}^{n}\frac{e^{-\frac{(s-s_i)^2}{2h^2}}}{\sqrt{2\pi}} \qquad (1)$$

where h is the bandwidth and s is the point for which the density is estimated.

As shown in (Botev et al., 2010), the construction of a kernel density estimator can be (from a mathematical perspective) compared to the process of computing the amount of heat generated when heat kernels are placed at each s_i sample point. Knowing that a heat kernel is the fundamental solution of the

Fourier heat equation, $\hat{f}(s)$ can be computed. The advantage of this approach is that it also introduces a plug-in bandwidth selection method which uses the asymptotic properties of the resulting $\hat{f}(s)$ estimator to compute the asymptotically optimal plug-in bandwidth h, without requiring any numerical optimization, thus speeding up the process of finding the promising parameter sets.

Because we are interested in finding the parameter sets that yield both a success and a low contact force between the bottle and the crate, a summation of the two KDE's (see Figure 7) is used for a better representation of the data and the search space. Finding the best parameter set means finding the maximum of the density surface. This can be done by applying optimization algorithms, such as gradient ascent. However, due to the nature of the data and because the density is represented by a matrix where its size is defined by the x and ϕ parameters and the individual density values depend on d, the best parameter set can be found by computing the maximum value of the matrix. The best parameter set is found to be [$3.5\,mm$, $5°$]. Visualizing the KDE data representation, we can observe that the density curve also has a second peak, around [$-10\,mm$, $-30°$]. These two peaks correspond to the main successful areas of the search space, represented in Figure 5(a) and Figure 5(c) and to the lower force areas, as shown in Figure 5(b) and Figure 5(d). The success of the PiH action drops in-between these two peaks due to the fact that the bottle gets stuck on the edge of the hole and also applies force on the crate.

4.2 Verification on Real System

Compared to the real world case, the simulator is more conservative because the slippage between the bottle and the plastic gripper or the compliance of the bottle, which can endure a big amount of deformation before actually breaking, are not considered in simulation. Both of these phenomenons can potentially lead to accidental successful trials, thus leading to a wrong prediction of the outcome.

Based on the results obtained in the previous subsection, a set of real world experiments were performed. The experiment starts with the visual servoing part, as described in 3.1, where the robot arm is moving the bottle towards the crate. Once the bottle is at the desired position, the PiH action is performed, using specified parameters as input (see Figure 8). Aside from executing the selected "best" parameter set, we also investigate 9 other sets, chosen manually from both promising and non-promising areas found by the simulation phase in an attempt to show that the real world results align with the ones found by simulation. Each of the sets is tested 10 times and evaluated manually. This means that the d value for each of the individual samples $s_i \in (s_1, s_2, \ldots, s_{100})$ has one of the following values:

$$d = \begin{cases} 0, & \text{if bottle fell from the gripper} \\ 1, & \text{if failure, with contact force} \\ 2, & \text{if success, with big contact force} \\ 3, & \text{if success, with medium contact force} \\ 4, & \text{if success, with small contact force} \\ 5, & \text{if success, with no contact force} \end{cases}$$

Following the method described in the previous subsection, we also apply KDE on the outcome of the real world experiments (see Figure 6(a)). Analyzing the KDE result, we can observe that the pattern of the density curve is similar to the one suggested by the simulation results in Figure 7. Additionally, the best parameter set - found to be [$3.5\,mm$, $5°$] by the simulator - had a success rate of 100% on the real platform. The parameter set [$-10\,mm$, $-30°$] corresponding to the second peak had a success rate of 70%, thus confirming the validity of the data. The [$-2.5\,mm$, $-15°$] and [$5\,mm$, $25°$] parameter sets also gave good results due to the compliance and curved shape of the bottle, which makes the insertion possible even if the edge of the hole is touched.

As mentioned, the robot is not equipped with a force-torque sensor. On order to verify that the assumption about the forces is correct, a third AR marker, was placed on the side of the crate. The idea is that, when force is applied, the crate is moved and thus the movement of the marker can be detected. Moreover, we verify if the scale of the movement is proportional to the strength of the contact force.

The translational movement of the AR marker is investigated by tracking how the length of the position vector (defined for the marker frame) changes over the course of the PiH action. Similarly, the rotation is checked by tracking the changes in quaternion angles during the action performance (see Figure 6(a)). The spikes in the translation and rotation appear at the moment any kind of contact force is applied. For the [$3.5\,mm$, $5°$] parameter set, we can see that there is only sub-millimeter and sub-degree movement, thus suggesting that no major force is applied to the crate. The registered movement is due to the fact that the marker can be correctly tracked only within millimeter precision, so anything bellow that will be affected by noise. The spikes that appear around the 460 mark are generated by the bottle falling into the crate hole when it is released from the gripper. On the other hand, for the [$10\,mm$, $-30°$] parameter set we can observe that when the bottle hits the edge of the crate, the tracker registers a movement of more than $3\,mm$ in translation and $2.5°$ degrees in rotation. This suggests that a bigger contact force is applied, which aligns with the force estimation results in Figure 5(d) and Figure 7.

4.3 Addition of Positional Noise

To further test the validity of the simulation results, we opt to make a series of real world experiments where we add extra positional uncertainty by not allowing the system to update the position of the crate before performing the PiH sequence. This means that the robot *blindly* performs the PiH action, assuming that the crate is placed in the correct position.

We investigate the same 10 parameter sets that were tested in 4.2, again with 10 trials for each (a total of 100 experiments). The results are shown in Figure 6(b). It can be observed that, while some peeks decrease compared to the case shown in Figure 6(a) due to the appearance of higher forces, the data is following a similar pattern to the one shown in the previous subsection and as estimated by the simulator. The best parameter set had again a success rate of 100%. However, the success rate of the $[-10\,mm, -30°]$ peak dropped to only 10%, thus proving that not being able to update the position of the crate has a huge impact on the success probability, even if the positional difference is less than a few millimeters.

The movement of the side marker is also tracked and the results are shown in Figure 6(b). For the *good* parameter set $[-2.5\,mm, -15°]$, little movement is registered by the tracker, thus suggesting that no major contact forces are applied on the crate during the PiH action execution. The peak at the 520 mark is due to the bottle dropping into the crate. For the $[-5\,mm, -35°]$ parameter set, a large movement of $1\,cm$ in translation is registered, which suggests that the crate was pushed hard with the bottle, once again confirming the force estimation results in Figure 5(d) and Figure 7. These results show that the robot will fail even when using some of the *good* parameter sets, if the positional error is larger than a few centimeters and if the system is not allowed to update and compensate for it, thus underlining the importance of considering the uncertainties when performing such a task.

5 FUTURE WORK

The presented method has shown that industrial solutions can be used and applied successfully with a service robot, in a home-like environment. Future research will have to consider other industrial tasks that could be adapted and used in similar service robotics scenarios. In addition, because some of these tasks are collaborative in nature, an investigation of the social implications of the human-robot interaction could be carried out.

6 CONCLUSIONS

In this paper an industrial-robotics inspired approach to solve the Peg-in-Hole task of inserting bottles into a crate is proposed. The work is performed using the Care-O-Bot service robot, without making use of additional, specialized sensors, calibration or compliant grippers. If we consider the parameterization of the PiH action, as described in 3.2, than the goal of the proposed method is to find the *best* parameter sets - i.e. parameters for which the PiH action yields both a successful insertion of the bottle and a low or non-existing contact force. The method starts by exploring the parameter search space. This is done by iteratively simulating the PiH action together with using a learning algorithm that takes into consideration the process uncertainties and the contact forces. Using Kernel Density Estimation, the parameter space is then reduced to a subset of *promising* parameters.

Making use of this knowledge, real world experiments are performed with the Care-O-Bot platform. 10 different parameter sets are selected from both *promising* and *non-promising* areas of the parameter space, as proposed by the learning algorithm, for which the PiH action is repeated for 10 times. We perform 200 experiments in two series - first by just running the action path and secondly by adding an additional position error, by not allowing the robot to update the position of the crate before performing the PiH action. Both experiment series showed that the real world results align with the ones found by the learning algorithm. More specifically, the *best* parameter set proposed by the learning component proved to have a success rate of 100%. This proves that adapting and applying solutions developed for the industrial robotics field is a viable option for service robotics, as long as the task uncertainties arising from the unstructured environment in which a service robot normally has to operate are taken into account.

ACKNOWLEDGEMENTS

This work was supported by Patient@home, funded by the Danish Innovation Fond, and Health-CAT, funded by European Regional Development Fund.

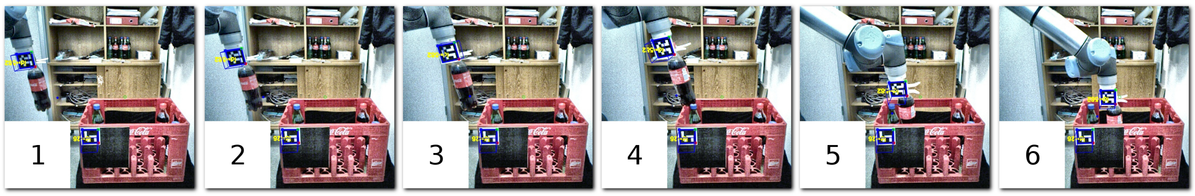

Figure 8: The full action sequence: visual servoing (1-4) and Peg-in-Hole (5-6).

REFERENCES

Berio, D., Calinon, S., and Leymarie, F. F. (2016). Learning dynamic graffiti strokes with a compliant robot. In *IEEE/RSJ Int. Conf. on Intelligent Robots and Systems*, pages 3981–3986.

Botev, Z. I., Grotowski, J. F., Kroese, D. P., et al. (2010). Kernel density estimation via diffusion. *The Annals of Statistics*, 38(5):2916–2957.

Cherubini, A., Chaumette, F., and Oriolo, G. (2008). A position-based visual servoing scheme for following paths with nonholonomic mobile robots. In *IEEE/RSJ Int. Conf. on Intelligent Robots and Systems*, pages 1648–1654.

Detry, R., Kraft, D., Kroemer, O., Bodenhagen, L., Peters, J., Krüger, N., and Piater, J. (2011). Learning grasp affordance densities. *Paladyn Journal of Behavioral Robotics*, 2(1).

Dietrich, F., Buchholz, D., Wobbe, F., Sowinski, F., Raatz, A., Schumacher, W., and Wahl, F. M. (2010). On contact models for assembly tasks: Experimental investigation beyond the peg-in-hole problem on the example of force-torque maps. In *IEEE/RSJ Int. Conf. on Intelligent Robots and Systems*, pages 2313–2318.

Gams, A. and Petrič, T. (2016). On-line modifications of robotic trajectories: Learning, coaching and force vs. position feedback. In *Int. Conf. on Robotics in Alpe-Adria Danube Region*, pages 20–28. Springer.

Gams, A., Petric, T., Nemec, B., and Ude, A. (2014). Learning and adaptation of periodic motion primitives based on force feedback and human coaching interaction. In *IEEE-RAS Int. Conf. on Humanoid Robots*, pages 166–171.

Garrido-Jurado, S., noz Salinas, R. M., Madrid-Cuevas, F., and Marín-Jiménez, M. (2014). Automatic generation and detection of highly reliable fiducial markers under occlusion. *Pattern Recognition*, 47(6):2280 – 2292.

Graf, B., Reiser, U., Hägele, M., Mauz, K., and Klein, P. (2009). Robotic home assistant care-o-bot 3 - product vision and innovation platform. In *IEEE Workshop on Advanced Robotics and its Social Impacts*.

Gratal, X., Romero, J., and Kragic, D. (2011). Virtual visual servoing for real-time robot pose estimation. *IFAC Proceedings Volumes*, 44(1):9017–9022.

Jørgensen, J. A. and Petersen, H. G. (2008). Usage of simulations to plan stable grasping of unknown objects with a 3-fingered Schunk hand. In *IEEE Int. Conf. on Intelligent Robots and Systems, Workshop - Robot simulators: available software, scientific applications and future trends*.

Kashiri, N., Laffranchi, M., Tsagarakis, N. G., Margan, A., and Caldwell, D. G. (2014). Physical interaction detection and control of compliant manipulators equipped with friction clutches. In *IEEE Int. Conf. on Robotics and Automation*, pages 1066–1071.

Kyrki, V., Kragic, D., and Christensen, H. I. (2004). New shortest-path approaches to visual servoing. In *IEEE/RSJ Int. Conf. on Intelligent Robots and Systems*, pages 349–354.

Lin, L. L., Yang, Y., Song, Y. T., Nemec, B., Ude, A., Rytz, J. A., Buch, A. G., Krüger, N., and Savarimuthu, T. R. (2014). Peg-in-hole assembly under uncertain pose estimation. In *Proc. of the 11th World Congress on Intelligent Control and Automation*, pages 2842–2847.

Mainprice, J., Hayne, R., and Berenson, D. (2015). Predicting human reaching motion in collaborative tasks using inverse optimal control and iterative re-planning. In *IEEE Int. Conf. on Robotics and Automation*, pages 885–892.

Schwarz, M., Schulz, H., and Behnke, S. (2015). RGB-D object recognition and pose estimation based on pre-trained convolutional neural network features. In *IEEE Int. Conf. on Robotics and Automation*, pages 1329–1335.

Sørensen, L. C., Buch, J. P., Petersen, H. G., and Kraft, D. (2016). Online action learning using kernel density estimation for quick discovery of good parameters for peg-in-hole insertion. In *13th Int. Conf. on Informatics in Control, Automation and Robotics*.

Zuiderveld, K. (1994). Contrast limited adaptive histogram equalization. In *Graphics gems IV*, pages 474–485. Academic Press Professional, Inc.